

Controlling the Shifting Degree of Interpenetrated Metal-Organic Frameworks by Modulator and Temperature and Their Hydrogen Adsorption Properties

Jingui Duan, Junfeng Bai, * Baishu Zheng, Yizhi Li, Wenchao Ren

State Key Laboratory of Coordination Chemistry, School of Chemistry and Chemical Engineering, Nanjing University, Nanjing 210093, PR China

Materials and methods

All the reagents and solvents were commercially available and used as received. The elemental analysis was carried out with a Perkin-Elmer 240C elemental analyzer. The FTIR spectra were recorded from KBr pellets in the range of 4000-400 cm⁻¹ on a VECTOR 22 spectrometer. Thermal analyses were performed on a Universal V3.9A TA Instruments from room temperature to 600°C with a heating rate of 10°C/min under flowing nitrogen. ¹H NMR spectra were recorded on a Bruker DRX-500 spectrometer at ambient temperature with tetramethylsilane as an internal reference. The powder X-ray diffraction patterns (PXRD) measurements were carried on a Bruker axs D8 Advance 40kV, 40mA for CuK_α(λ = 1.5418 Å) with a scan rate of 0.2s/deg at room temperature. Simulation of the PXRD spectra was obtained by the single-crystal data and diffraction-crystal module of the *Mercury* program.

Synthesis and general characterizations

Synthesis of H₂L: The ligand of H₂L was synthesized from 4-Chlorocarbonyl-benzoic acid and 4-Amino-benzoic acid according to a method reported by Cavalleri et al.¹ Anal. Calcd. C₁₅H₁₁NO₅: C, 63.16; H, 3.89; N, 4.91%. Found: C, 63.12; H, 3.90; N, 4.89%. m.p.: >330°C. IR(KBr, pellet, cm⁻¹): 3317(s), 1686 (s), 1646 (s), 1606 (s), 1572 (s), 1522(s) 1426(s), 1293(w), 1175(s), 935(s), 876(s), 783(s), 695(s), 555(s), 528(s). ¹H NMR (400 MHz, MeOD): δ = 7.952 (m, 4H), 8.075 (m, 4H), 10.690(s, 1H).

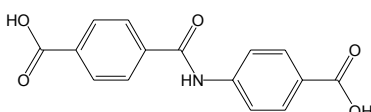


Fig. S1 The structure of H₂L

Synthesis of NJU-Bai1 and NJU-Bai2:

For NJU-Bai1: a mixture of H₂L(20mg, 0.07mmol) and Zn(NO₃)₂·6H₂O (62mg, 0.21mmol) was suspended in 2ml DMF and heated in a sealed vial (20ml) at 80°C for 48h, then cooled to room temperature. Colorless cubic crystals were collected. Yield: 42.1%. The evacuated NJU-Bai1 was formulated as C₄₅H₂₇N₃O₁₆Zn₄: C, 47.95; H, 2.41; N, 3.73%. Found: C, 47.32; H, 2.11; N, 3.91%. IR (cm⁻¹): 3377 (s), 1662 (s), 1602(m), 1521 (s), 1397 (m), 1321 (s), 1179 (w), 1106(w), 782(s), 625(s).

For NJU-Bai2: a mixture of H₂L(20mg, 0.07mmol), L-Tyrosine (12mg, 0.07mmol) and Zn(NO₃)₂·6H₂O (62mg, 0.21mmol) was suspended in 2ml DMF and heated in a sealed vial

(20ml) at 110°C for 48h, then cooled to room temperature. Grayish cubic crystals were collected. Yield: 52.8%. The evacuated NJU-Bai2 was formulated as C₄₅H₂₇N₃O₁₆Zn₄: C, 47.95; H, 2.41; N, 3.73%. Found: C, 47.58; H, 1.98; N, 4.18%. IR (cm⁻¹): 3358 (s), 1655 (s), 1602(m), 1536 (s), 1377 (m), 1326 (s), 1179 (w), 1103(s), 899(s), 782(s), 663(s).

X-ray crystallography

Single-crystal X-ray diffraction data were measured on a Bruker Smart Apex CCD diffractometer at 298 K using graphite monochromated Mo/K α radiation ($\lambda = 0.71073 \text{ \AA}$). Data reduction was made with the Bruker Saint program. The structures were solved by direct methods and refined with full-matrix least squares technique using the SHELXTL package². Non-hydrogen atoms were refined with anisotropic displacement parameters during the final cycles. Organic hydrogen atoms were placed in calculated positions with isotropic displacement parameters set to $1.2 \times U_{eq}$ of the attached atom. The unit cell includes a large region of disordered solvent molecules, which could not be modeled as discrete atomic sites. We employed PLATON/SQUEEZE³ to calculate the diffraction contribution of the solvent molecules, then, to produce a set of solvent-free diffraction intensities; structures were then refined again using the data generated. CCDC 7935587 - 792558 for NJU-Bai1 and NJU-Bai2 contain the supplementary crystallographic data for this paper. These data can be obtained free of charge from the Cambridge Crystallographic Data Centre via www.ccdc.cam.ac.uk/data_request/cif. Crystal data are summarized in Table S1.

Gas Sorption Measurements

In the gas sorption measurement, Ultra-high-purity grade, N₂ and H₂ (>99.999%) were used throughout the adsorption experiments. All of the measured sorption isotherms have been repeated several times to confirm the reproducibility within experimental error.

Low pressure gas sorption measurements: Low-pressure N₂ and H₂ adsorption measurements (up to 1 bar) were performed on Micromeritics ASAP 2020 M+C surface area analyzer. About 70 mg of samples were activated at 140 °C for 30 hours by using the “outgas” function of the surface area analyzer. Helium was used for the estimation of the dead volume, assuming that it is not adsorbed at any of the studied temperatures. To provide high accuracy and precision in determining P/P₀, the saturation pressure P₀ was measured throughout the N₂ analyses by means of a dedicated saturation pressure

transducer, which allowed us to monitor the vapor pressure for each data point. A part of the N₂ sorption isotherm in the P/P₀ range 0.05–0.3 was fitted to the BET equation to estimate the BET surface area and the Langmuir surface area calculation was performed using all data points. The pore size distribution was obtained from the H-K (micro-pore) and BJH (meso-pore) method in the Micromeritics ASAP2020 software package based on the N₂ sorption at 77K.

High pressure gravimetric gas sorption measurements: High pressure adsorption of H₂ was measured using an IGA-003 gravimetric adsorption instrument (Hiden-Isochema, UK) over a pressure range of 0-20 bar at 77 K.

Table S1 Crystal data and structure refinement for NJU-Bai1 and NJU-Bai2

	NJU-Bai1	NJU-Bai2
Empirical formula	C ₄₅ H ₅₁ N ₃ O ₂₈ Zn ₄	C ₅₁ H ₃₈ N ₅ O ₁₈ Zn ₄
Formula weight	1343.45	1270.43
Space group	I23	P21/c
a/Å	19.2919(14)	19.0893(15)
b/Å	19.2919(14)	26.952(2)
c/Å	19.2919(14)	31.7133(18)
β /°	90	119.592(3)
V/Å ³	7180.0(9)	14188.1(18)
Z	2	4
Dcalc/gcm ⁻³	0.621	0.595
μ/mm ⁻¹	0.695	0.697
Θ range°	1.5 - 28.0	1.1 - 26.0
Index ranges	-17 ≤ h ≤ 17 -17 ≤ k ≤ 18 -25 ≤ l ≤ 25	-23 ≤ h ≤ 20 -33 ≤ k ≤ 33 -33 ≤ l ≤ 39
R1,wR2a[I>2σ(I)]	0.0541, 0.1643	0.0614, 0.1428
GOF	1.055	1.074

Table S2 Bond Distances and Bond Angles of NJU-Bai1 and NJU-Bai2

1			
Zn1-O1	1.9651(4)	Zn1-O2g	1.901(2)
Zn1-O2	1.901(2)	Zn1-O2l	1.901(2)
O1-Zn1-O2	108.54(7)	O2-Zn1-O2g	110.38(9)
O1-Zn1-O2g	108.54(7)	O2-Zn1-O2l	110.38(9)
O1-Zn1-O2l	108.54(7)	O2g-Zn1-O2l	110.38(9)
2			
Zn1-O1	1.930(2)	Zn1-O12	1.970(2)
Zn1-O2	1.914(3)	Zn1-O16	2.061(2)
Zn2-O1	1.916(2)	Zn2-O8	1.946(2)
Zn2-O13	1.959(2)	Zn2-O6-	1.862(3)
Zn3-O1	1.979(2)	Zn3-O3	2.491(2)
Zn3-O7	2.084(2)	Zn3-O11	2.045(2)
Zn3-O17	2.003(2)	Zn3-O18	2.163(2)
Zn4-O1	1.925(2)	Zn4-O10	1.938(2)
Zn4-O15	1.843(2)	Zn4-O5-	1.953(3)
O1-Zn1-O2	121.34(9)	O1-Zn3-O18	83.49(8)
O1-Zn1-O12	109.71(9)	O3-Zn3-O7	89.98(7)
O1-Zn1-O16	112.52(9)	O3-Zn3-O11	170.80(9)
O2-Zn1-O12	108.39(9)	O3-Zn3-O17	79.97(8)
O2-Zn1-O16	101.94(9)	O3-Zn3-O18	85.14(7)
O12-Zn1-O16	100.85(8)	O7-Zn3-O11	95.58(8)
O1-Zn2-O8	119.78(9)	O7-Zn3-O17	88.18(9)
O1-Zn2-O13	114.28(9)	O7-Zn3-O18	174.29(9)
O1-Zn2-O6_a	108.80(9)	O11-Zn3-O17	92.85(9)
O8-Zn2-O13	97.64(8)	O11-Zn3-O18	88.90(8)
O6_a-Zn2-O8	110.42(10)	O17-Zn3-O18	88.06(9)
O6_a-Zn2-O13	104.63(10)	O1-Zn4-O10	117.22(9)
O1-Zn3-O3	84.53(8)	O1-Zn4-O5_a	111.98(9)
O1-Zn3-O7	99.01(9)	O10-Zn4-O15	111.96(8)
O1-Zn3-O11	101.78(9)	O5_a-Zn4-O10	103.24(9)
O1-Zn3-O17	162.92(9)	O5_a-Zn4-O15	102.57(10)

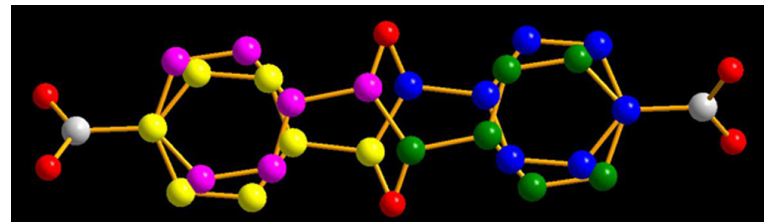


Fig. S2 The disorder of ligand unit in NJU-Bai1. The different colors show four possible orientations in the framework. The symmetry transformation used to generate equivalent atoms: (yellow) x, y, z ; (pink) $2-x, y, 2-z$; (green) $x, 1-y, 2-z$; (blue) $2-x, 1-y, z$.

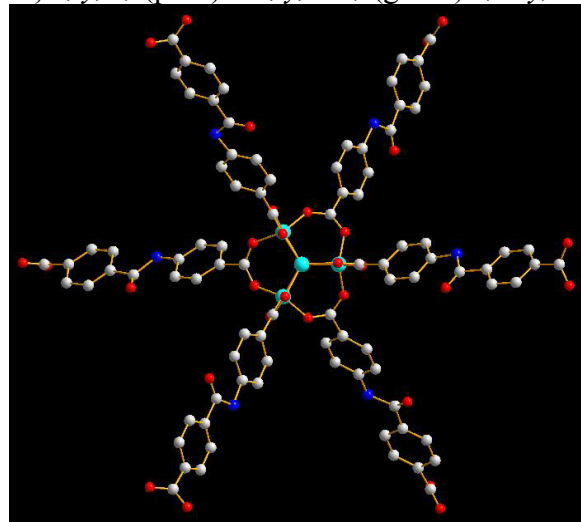


Fig. S3 The Zn_4O cluster was connected by six ligand units in NJU-Bai1.

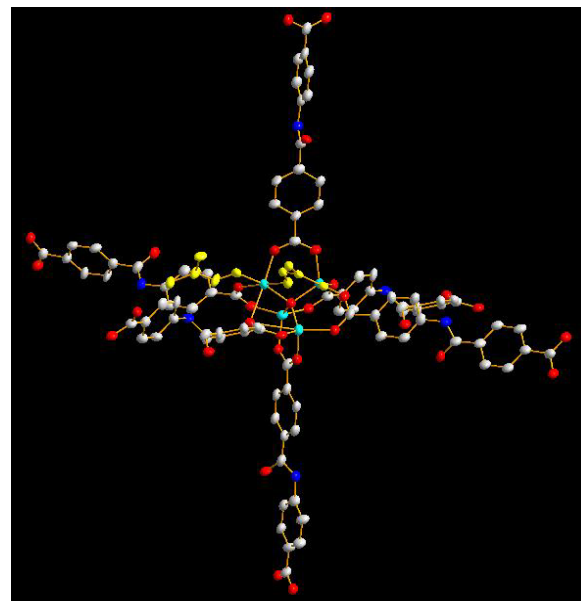


Fig. S4 The Zn_4O cluster was connected by six ligand units and two DMF molecules (yellow atoms) in NJU-Bai2.

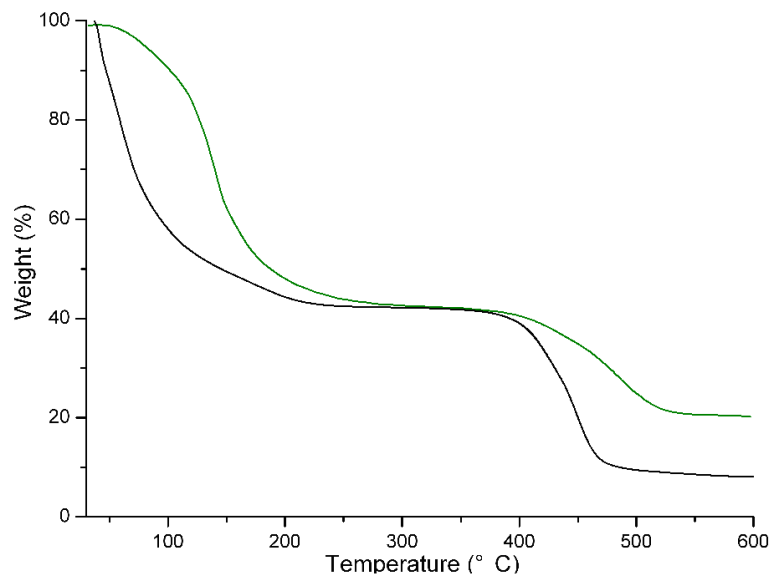


Fig. S5 TG curves of NJU-Bai1 (black) and NJU-Bai2 (green).

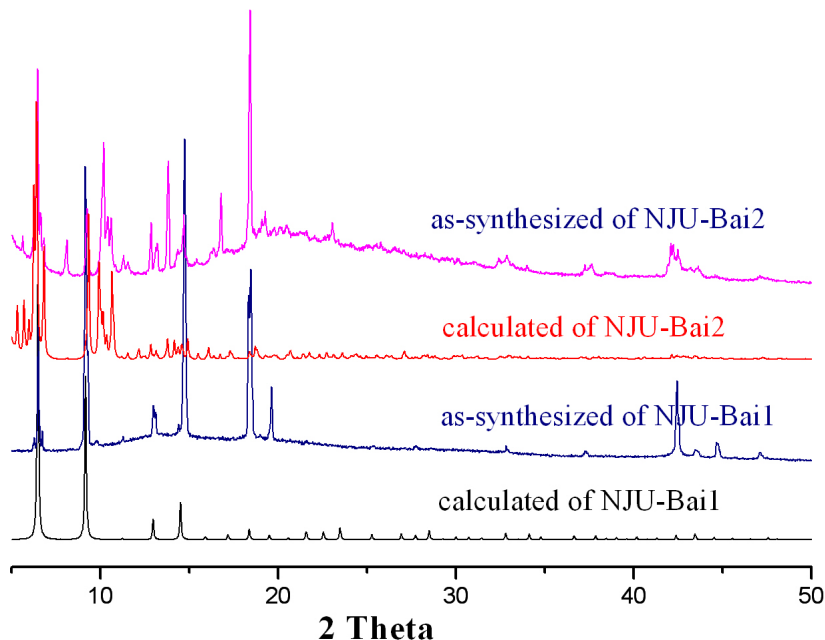


Fig. S6 Powder X-ray diffraction (PXRD) patterns of NJU-Bai1 and NJU-Bai2.

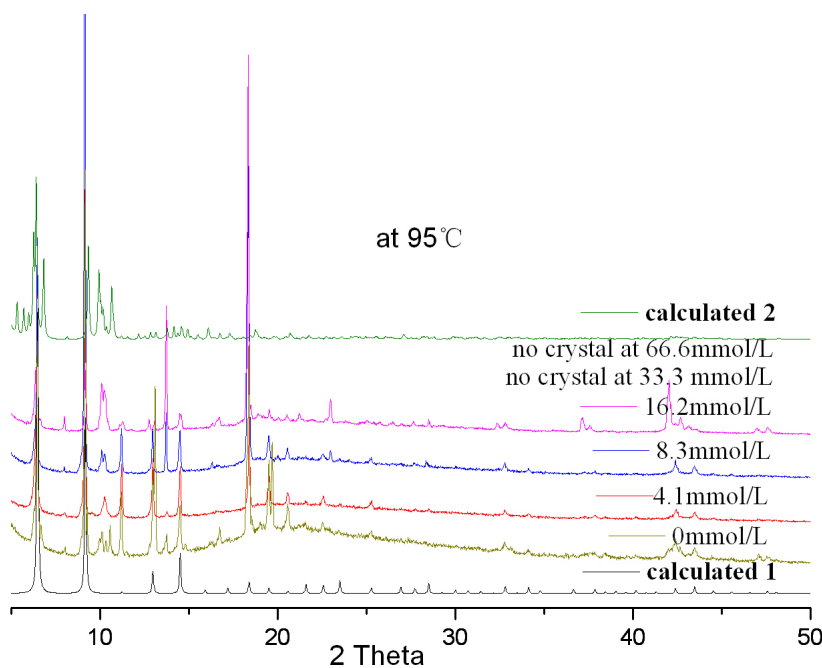


Fig. S7 Comparison of PXRD patterns of products at different concentration of L-Tyrosine at 95 °C.

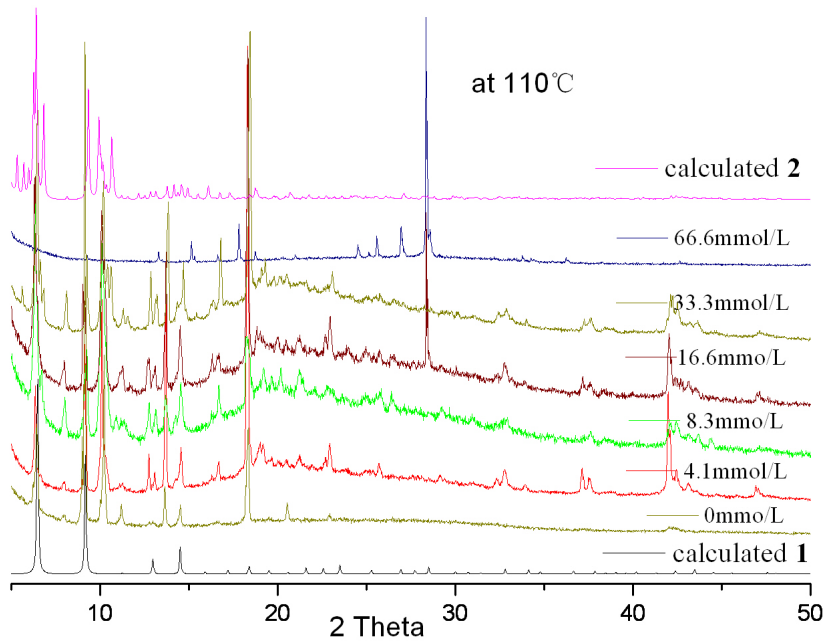


Fig. S8 Comparison of PXRD patterns of products at different concentration of L-Tyrosine at 110°C.

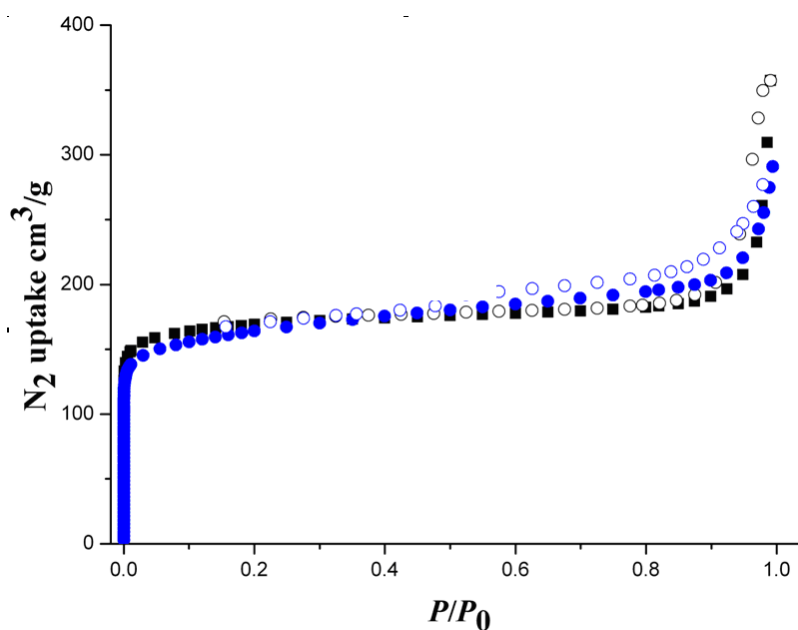


Fig. S9 N₂ adsorption isotherms of NJU-Bai1 (blue) and NJU-Bai2 (black) at 77K.

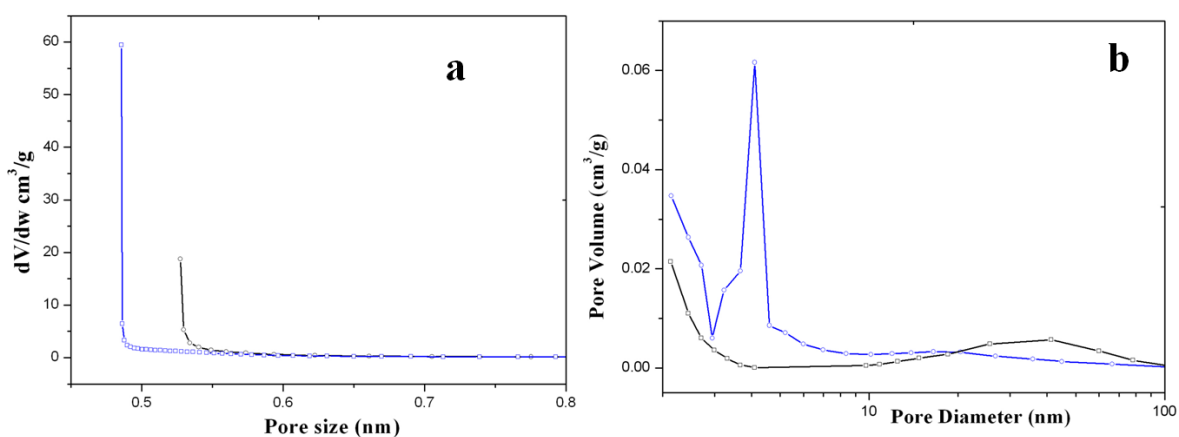


Fig. S10 The calculated pore size distributions (a: micro-pores; b: meso-pores) of NJU-Bai1 (blue) and NJU-Bai2 (black) at 77K.

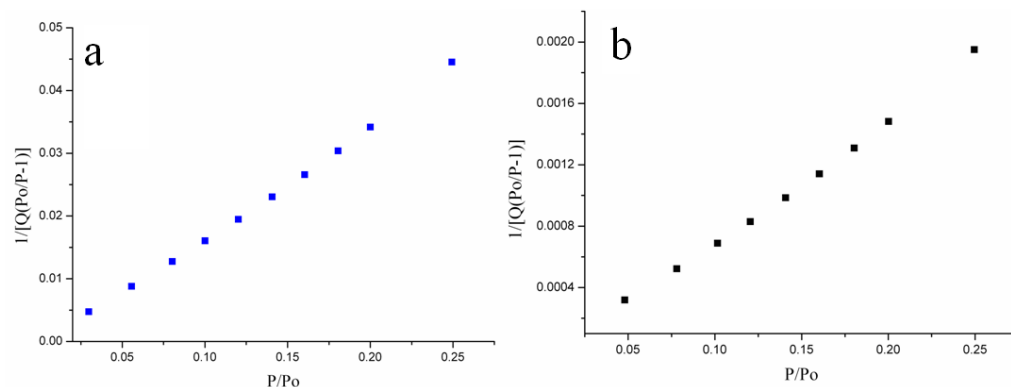


Fig. S11 The BET plot calculated from N₂ uptake isotherms of NJU-Bai1 (a) and NJU-Bai2 (b).

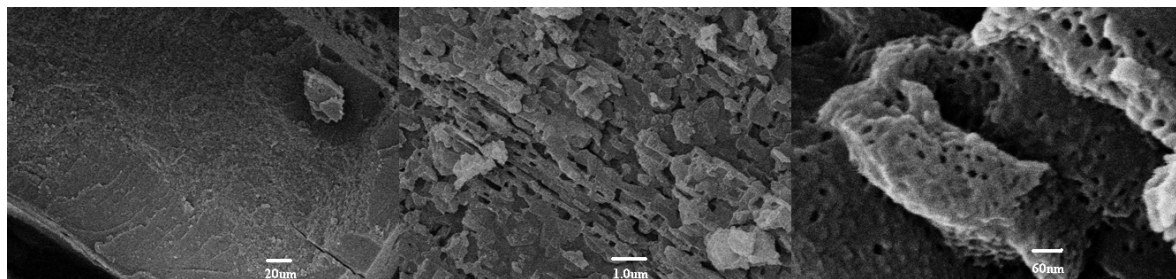


Fig. S12 The SEM of evacuated sample of NJU-Bai1 shows the existence of mesopores.

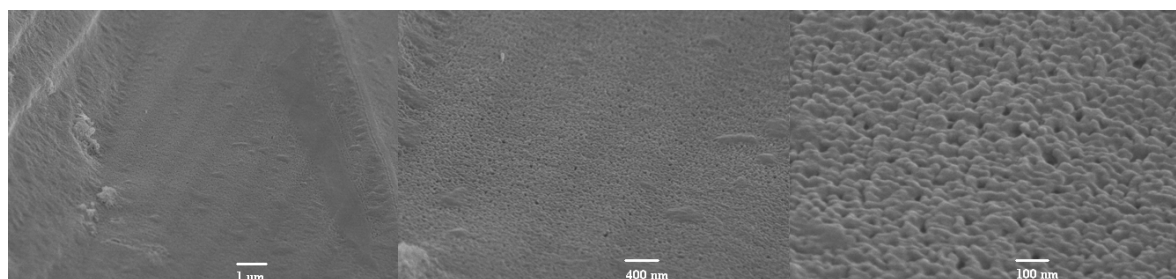


Fig. S13 The SEM of evacuated sample of NJU-Bai2 shows the existence of mesopores.

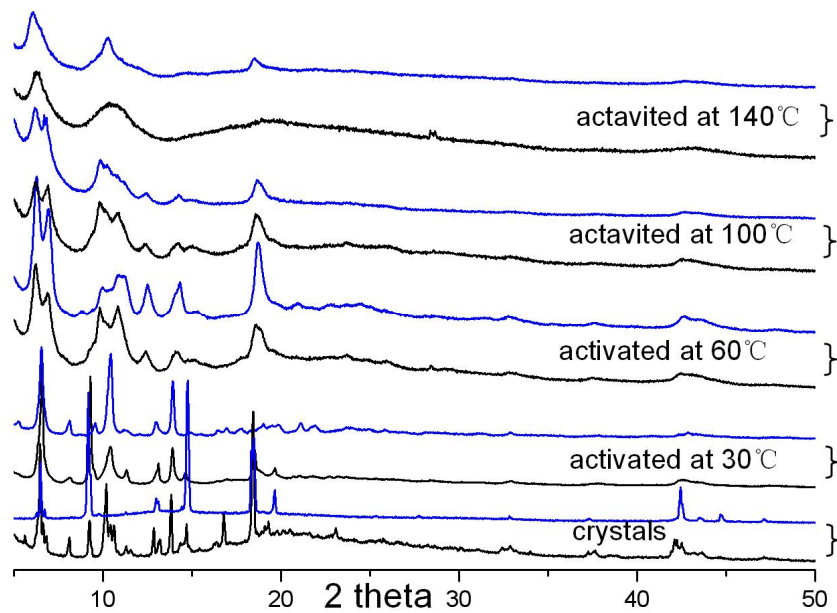


Fig. S14 PXRD patterns of evacuated frameworks of NJU-Bai1 (blue) and NJU-Bai2 (black) dried in vacuum for 10h at different temperature.

References:

1. P. Cavalleri, N. N. Chavan, A. Ciferri, C. DellErba, A. E. Lozano, M. Novi and J. Preston, *Macromolecules*, 1997, **30**, 3112.
2. G. M. Sheldrick, *Acta Crystallogr. Sect. A*, 2008, **64**, 112.
3. A. L. Spek, *J. Appl. Crystallogr.*, 2003, **36**, 7.